

Supporting Information

Unraveling the evolution of exsolved Fe-Ni alloy nanoparticles in Ni-doped $\text{La}_{0.3}\text{Ca}_{0.7}\text{Fe}_{0.7}\text{Cr}_{0.3}\text{O}_{3-\delta}$ and their role in enhancing $\text{CO}_2\text{-CO}$ electrocatalysis

Haris Masood Ansari,^a Adam Stuart Bass,^a Nabeel Ahmad,^b and Viola I. Birss^{*a}

^aDepartment of Chemistry, University of Calgary, 2500 University Dr. NW, Calgary, AB T3G5V2, Canada,

*Email: birss@ucalgary.ca

^bRosalind Franklin Institute, Harwell Campus, Didcot, OX11 0FA, UK

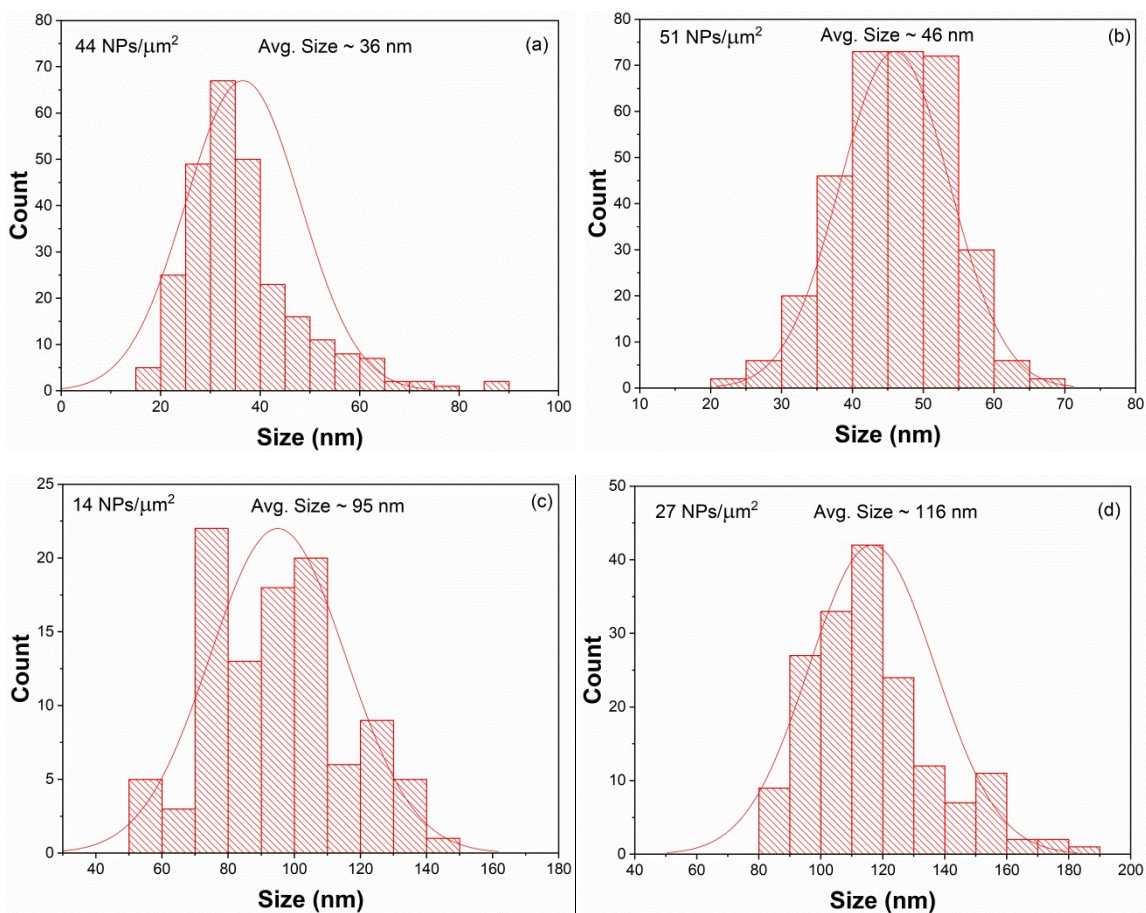


Fig. S1 Histograms depicting the size distribution and areal densities of the NPs grown in 5:95 $\text{H}_2\text{:N}_2$ at (a) 750 °C for 5 hr, (b) 750 °C for 25 hr, (c) 800 °C for 5 hr, and (d) 800 °C for 25 hr, respectively.

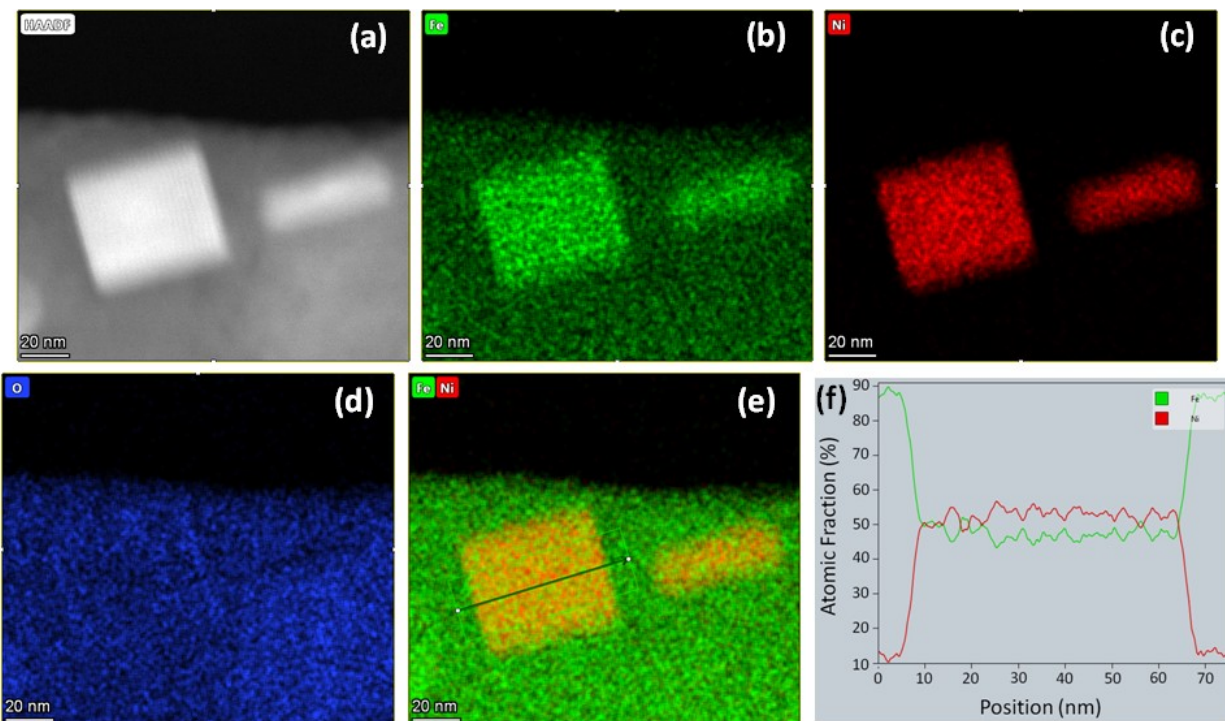


Fig. S2 (a) HAADF STEM image of a faceted NP with a square base. EDS elemental maps of (b) Fe, (c) Ni, and (d) O, and (e) Fe and Ni overlaid, for the NP in (a). (f) EDS line scan across the middle of the NP in (d) showing a stoichiometry close to FeNi. The LCFCrN powder was reduced at 750 °C for 5 hr in 5:95 H₂:N₂.

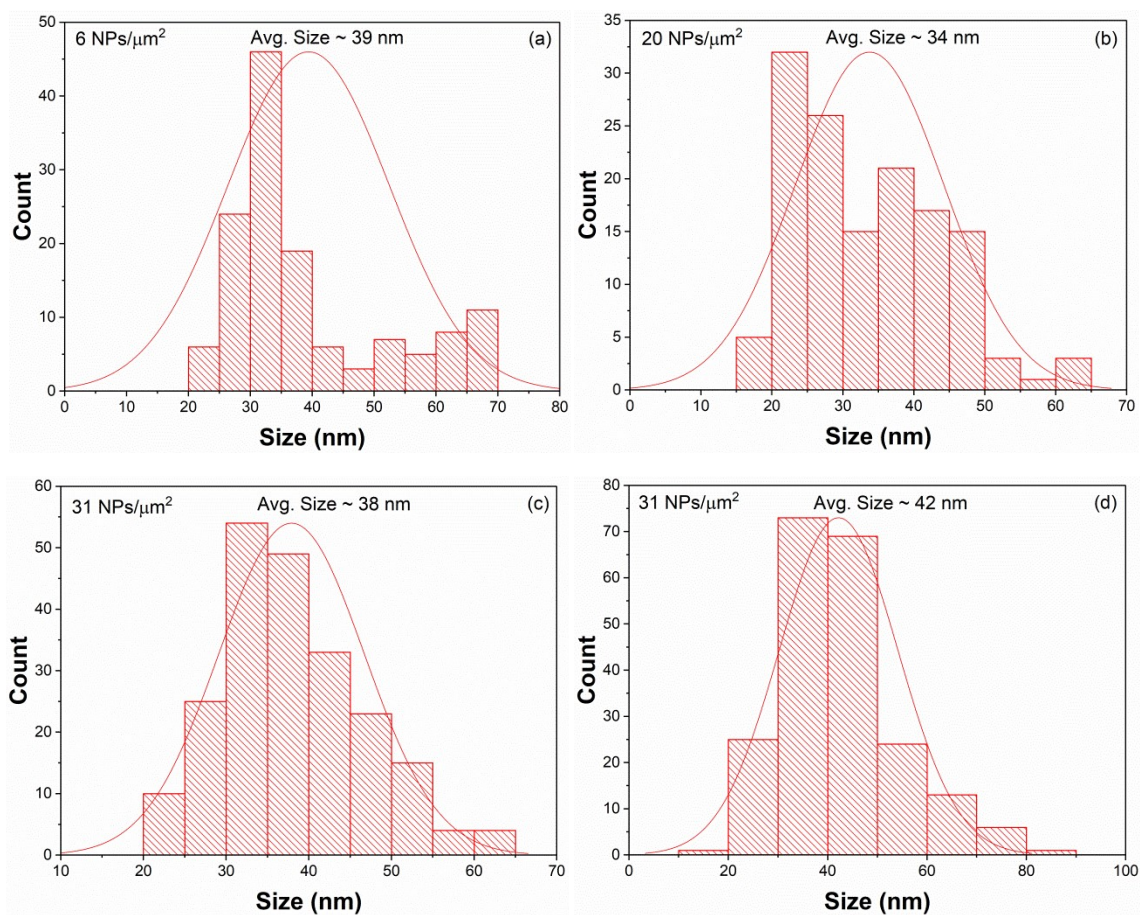


Fig. S3 Histograms depicting the size distribution and areal densities of the NPs grown at 800 °C for 5 hr for CO:CO₂ gas compositions of (a) 10:90, (b) 30:70, (c) 70:30, and (d) 90:10, respectively.

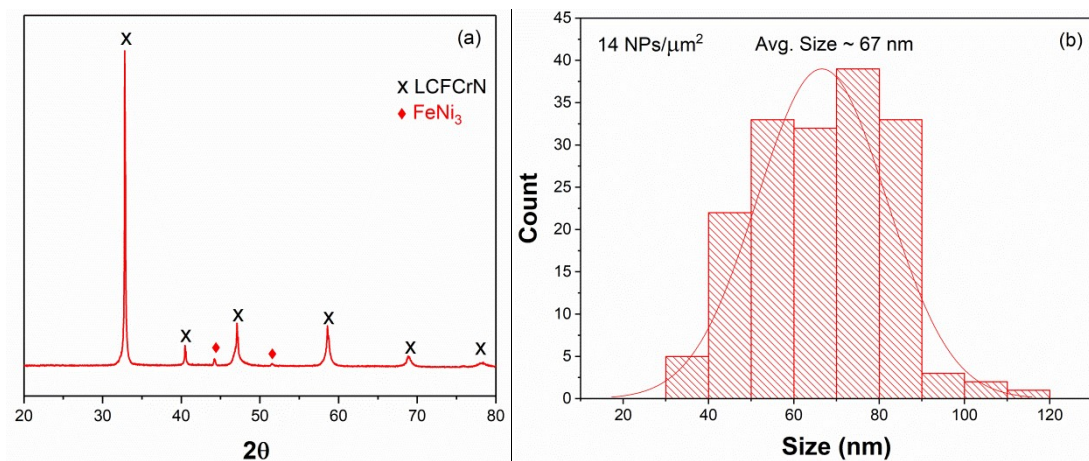


Fig. S4 (a) Room temperature x-ray diffraction pattern, and (b) a histogram depicting the size distribution and areal density of the NPs in LFCrN exposed to humidified 7.5% H_2 :92.5% N_2 at 800 °C for 5 hr.

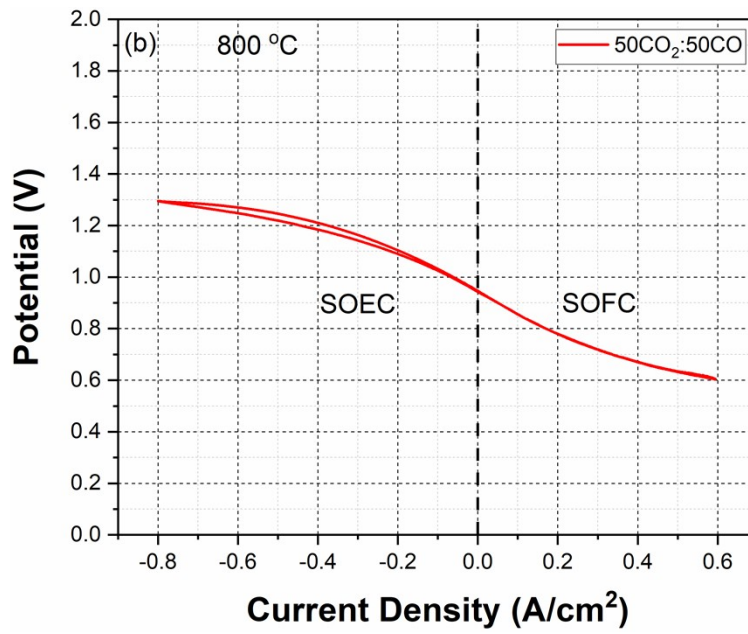


Fig. S5 (a) *iR* corrected CV acquired at 800 °C in a 50:50 CO₂:CO gas mixture.

Table S1. pO_2 of the gas compositions used in this work

Gas Composition	pO_2 (atm)
5:95 H ₂ :N ₂	$< 10^{-23}$
Humidified 7.5:92.5 H ₂ :N ₂	7.0×10^{-20}
5:95 CO:CO ₂	1.4×10^{-16}
10:90 CO:CO ₂	3.1×10^{-17}
30:70 CO:CO ₂	2.1×10^{-18}
50:50 CO:CO ₂	3.8×10^{-19}
70:30 CO:CO ₂	6.9×10^{-20}
90:10 CO:CO ₂	4.7×10^{-21}
95:5 CO:CO ₂	1.0×10^{-21}

Table S2. Performance comparison of various electrocatalysts for CO₂ reduction at 800 °C.

Fuel Electrode	Electrolyte/Oxygen Electrode	Cell Voltage (V)	Gas Atmosphere	Current Density (A/cm ²)	Ref.
Fe-Ni@LCFCrN	SSZ/LCFCrN	1.6	CO ₂	-0.65	This work
FeNi ₃ @SFMN-GDC	LSGM/LSCF-GDC	1.6	CO ₂	-0.93	[1]
SFMN-GDC	LSGM/LSCF-GDC	1.6	CO ₂	-0.63	[1]
LSFV-GDC	YSZ/ LSM-YSZ	1.6	CO ₂	-0.62	[2]
Ni@LSTMN-SDC	YSZ/LSM	1.6	CO ₂	-0.54	[3]
Fe-Ni@LSFN-GDC	YSZ/LSCF-GDC	1.6	70:30 CO ₂ :CO	-0.66	[4]

Note that our perovskite material (LCFCrN) is the only one that has not been composited with GDC or SDC, done by others to increase the ionic conductivity.

References

1. H. Lv, L. Lin, X. Zhang, D. Gao, Y. Song, Y. Zhou, Q. Liu, G. Wang, X. Bao, In Situ Exsolved FeNi₃ Nanoparticles on Nickel Doped Sr₂Fe_{1.5}Mo_{0.5}O_{6-δ} Perovskite for Efficient Electrochemical CO₂ Reduction Reaction, *J. Mater. Chem. A*, 2019, **7**, 11967-11975.
2. Y. Zhou, Z. Zhou, Y. Song, X. Zhang, F. Guan, H. Lv, Q. Liu, S. Miao, G. Wang, X. Bao, Enhancing CO₂ Electrolysis Performance with Vanadium-Doped Perovskite Cathode in Solid Oxide Electrolysis Cell, *Nano Energ.*, 2018, **50**, 43-51.
3. L. Ye, M. Zhang, P. Huang, G. Guo, M. Hong, C. Li, J. T. S. Irvine, K. Xie, Enhancing CO₂ Electrolysis through Synergistic Control of Non-Stoichiometry and Doping to Tune Cathode Surface Structures, *Nat. Commun.*, 2017, **8**, 14785.
4. S. Liu, Q. Liu, J.-L. Luo, Highly Stable and Efficient Catalyst with in Situ Exsolved Fe-Ni Alloy Nanospheres Socketed on an Oxygen Deficient Perovskite for Direct CO₂ Electrolysis, *ACS Catal.*, 2016, **6**, 6219-6228.